



From Disorder to Order in Marching Locusts

J. Buhl, *et al.*

Science **312**, 1402 (2006);

DOI: 10.1126/science.1125142

The following resources related to this article are available online at www.sciencemag.org (this information is current as of November 23, 2007):

Updated information and services, including high-resolution figures, can be found in the online version of this article at:

<http://www.sciencemag.org/cgi/content/full/312/5778/1402>

Supporting Online Material can be found at:

<http://www.sciencemag.org/cgi/content/full/312/5778/1402/DC1>

A list of selected additional articles on the Science Web sites **related to this article** can be found at:

<http://www.sciencemag.org/cgi/content/full/312/5778/1402#related-content>

This article **cites 26 articles**, 5 of which can be accessed for free:

<http://www.sciencemag.org/cgi/content/full/312/5778/1402#otherarticles>

This article has been **cited by** 13 article(s) on the ISI Web of Science.

This article has been **cited by** 6 articles hosted by HighWire Press; see:

<http://www.sciencemag.org/cgi/content/full/312/5778/1402#otherarticles>

This article appears in the following **subject collections**:

Psychology

<http://www.sciencemag.org/cgi/collection/psychology>

Information about obtaining **reprints** of this article or about obtaining **permission to reproduce this article** in whole or in part can be found at:

<http://www.sciencemag.org/about/permissions.dtl>

the C-terminal TonB domain. We do not observe TonB $\beta 4$ in our structure. Instead, the C terminus of TonB extends away from the complex, such that the FhuA Ton box forms a parallel β interaction with TonB $\beta 3$ (Fig. 2C). This observation clearly demonstrates that the complexation of TonB to FhuA occurs via strand exchange.

Our in vitro surface plasmon resonance studies (12, 13) indicated that TonB-FhuA complexation involves a kinetically limiting conformational rearrangement. The present structure showing exchange of TonB $\beta 4$ with the FhuA Ton box corroborates these biophysical observations and suggests that formation of the interprotein β sheet is the initial committed step of TonB-FhuA complexation. The complex that we observe in this structure is likely the 1:1 high-affinity complex identified by biophysical methods. Interactions between a FhuA Ton box peptide and residues from TonB $\beta 3$ and $\beta 4$ were recently reported (5). Ton box residues may therefore form low-affinity encounter interactions with TonB $\beta 3$ and $\beta 4$ before formation of the stable interprotein β sheet. TonB Gln¹⁶⁰ likely participates in these encounter interactions, perhaps facilitating displacement of TonB $\beta 4$. A cysteine cross-linking study (14) mapped a complex network of interactions between TonB residues 159 and 164 such that each TonB residue interacted with multiple residues in the BtuB Ton box. This is consistent with TonB residues at or near Gln¹⁶⁰ being involved in multiple transient encounter interactions before high-affinity complex formation.

The TonB-FhuA interface has a mean interfacial accessible surface area (Δ ASA) (15) of 1299 Å². The calculated shape correlation statistic (S_c) for this interface is 0.60, indicating that it has a surface complementarity similar to that observed for cork-barrel interfaces of TonB-dependent OM receptors (16). The TonB-FhuA interface is composed of a network of 17-residue pairs bound by hydrophilic interactions (table S2). All pairs were observed to have well-defined electron density for both FhuA and TonB side chains. Within this interface, a single electrostatic interaction occurs between FhuA cork residue Glu⁵⁶ and TonB Arg¹⁶⁶, located on TonB $\alpha 1$ (Fig. 3). A hydrogen bond is also formed between TonB Arg¹⁶⁶ and the main-chain carbonyl oxygen atom of FhuA Ala²⁶, located in the switch helix region. Ferrichrome binding to FhuA was previously observed to result in a 17.3 Å translocation of the FhuA N terminus and unwinding of the switch helix (9). Therefore, it appears that unwinding of the FhuA switch helix upon ligand binding occurs in order to stabilize FhuA interactions with TonB Arg¹⁶⁶. FhuA barrel residues Ala⁵⁹¹ and Asn⁵⁹⁴, located in or near periplasmic turn 8, also form hydrogen bonds with TonB Arg¹⁶⁶.

What does the crystal structure of the TonB-FhuA complex tell us about interactions of TonB with a cognate OM receptor and the transport of metal-chelated siderophore? Given our structural data, combined with findings from previous studies

of TonB interactions with OM receptors in vitro and in vivo, we propose that the interprotein β sheet formed between the receptor Ton box and the TonB C-terminal domain is required to position TonB helix $\alpha 1$ proximal to the receptor cork domain. In the TonB-FhuA structure, this results in TonB Arg¹⁶⁶ forming an electrostatic interaction with FhuA cork residue Glu⁵⁶. Both TonB Arg¹⁶⁶ (17) and FhuA Glu⁵⁶ located in the TEE motif (16) are highly conserved residues, predicting functional importance of this TonB-FhuA ionic interaction. Molecular dynamics simulations of FhuA have suggested that cork domain solvation may lower the energy barrier for active transport of ferrichrome (18). It has recently been proposed that hydration of the central β sheet of the cork domain may render it prone to disruption by TonB through transmission of a relatively small force perpendicularly applied to the β strands of the cork domain (16). Given its position proximal to the central β sheet of the FhuA cork domain, TonB Arg¹⁶⁶ is positioned to mediate a mechanical shearing or pulling force applied in trans to the central β sheet of the cork domain, resulting in its disruption. Localized unfolding of the cork domain would allow siderophore translocation into the periplasm, facilitating subsequent steps of the siderophore transport cycle.

References and Notes

1. C. Wandersman, P. Deleplaire, *Annu. Rev. Microbiol.* **58**, 611 (2004).
2. A. D. Ferguson, J. Deisenhofer, *Cell* **116**, 15 (2004).
3. C. Chang, A. Mooser, A. Plückthun, A. Wlodawer, *J. Biol. Chem.* **276**, 27535 (2001).
4. J. Ködding *et al.*, *J. Biol. Chem.* **280**, 3022 (2005).
5. R. S. Peacock, A. M. Weljie, S. P. Howard, F. D. Price, H. J. Vogel, *J. Mol. Biol.* **345**, 1185 (2005).
6. D. P. Chimento, A. K. Mohanty, R. J. Kadner, M. C. Wiener, *Nat. Struct. Biol.* **10**, 394 (2003).
7. A. D. Ferguson *et al.*, *Science* **295**, 1715 (2002).
8. S. K. Buchanan *et al.*, *Nat. Struct. Biol.* **6**, 56 (1999).
9. A. D. Ferguson, E. Hofmann, J. W. Coulton, K. Diederichs, W. Welte, *Science* **282**, 2215 (1998).

10. K. P. Locher *et al.*, *Cell* **95**, 771 (1998).
11. Materials and methods are available as supporting information on Science Online.
12. C. M. Khursigara, G. De Crescenzo, P. D. Pawelek, J. W. Coulton, *Biochemistry* **44**, 3441 (2005).
13. C. M. Khursigara, G. De Crescenzo, P. D. Pawelek, J. W. Coulton, *Protein Sci.* **14**, 1266 (2005).
14. N. Cadieux, C. Bradbeer, R. J. Kadner, *J. Bacteriol.* **182**, 5954 (2000).
15. S. Jones, J. M. Thornton, *Proc. Natl. Acad. Sci. U.S.A.* **93**, 13 (1996).
16. D. P. Chimento, R. J. Kadner, M. C. Wiener, *Proteins* **59**, 240 (2005).
17. R. A. Larsen *et al.*, *J. Bacteriol.* **178**, 1363 (1996).
18. J. D. Faraldo-Gómez, G. R. Smith, M. S. Sansom, *Biophys. J.* **85**, 1406 (2003).
19. We thank A. Berghuis (McGill University, Montreal, Quebec) and M. Cygler (Biotechnology Research Institute, National Research Council, Montreal, Quebec) for access to home source x-rays and for helpful discussions. F. Rotella and S. L. Ginell at the Advanced Photon Source, beamline 19-ID, assisted with data collection. Use of the Argonne National Laboratory Structural Biology Center beamlines at the Advanced Photon Source was supported by the U.S. Department of Energy, Office of Biological and Environmental Research, under Contract No. W-31-109-ENG-38. We acknowledge the suggestions of K. Diederichs (Universität Konstanz, Germany) concerning site-directed mutagenesis to improve crystal contacts of FhuA. Critical reviews of this manuscript were provided by A. Berghuis, H. Le Moual, and B. Nagar, all at McGill University; J. A. Kashul edited the document. This work was supported by operating grant MOP-14133 (to J.W.C.) from the Canadian Institutes of Health Research. Infrastructure from Canada Foundation for Innovation was awarded to the Montreal Integrated Genomics Group for Research on Infectious Pathogens. Coordinates and structure factors have been deposited in the Protein Data Bank (PDB) with the accession code 2GRX.

Supporting Online Material

www.sciencemag.org/cgi/content/full/312/5778/1399/DC1
Materials and Methods
SOM Text
Figs. S1 and S2
Tables S1 and S2
References

29 March 2006; accepted 27 April 2006
10.1126/science.1128057

From Disorder to Order in Marching Locusts

J. Buhl,^{1,2*} D. J. T. Sumpter,¹ I. D. Couzin,^{1,3} J. J. Hale,¹ E. Despland,^{1†} E. R. Miller,¹ S. J. Simpson^{1,2}

Recent models from theoretical physics have predicted that mass-migrating animal groups may share group-level properties, irrespective of the type of animals in the group. One key prediction is that as the density of animals in the group increases, a rapid transition occurs from disordered movement of individuals within the group to highly aligned collective motion. Understanding such a transition is crucial to the control of mobile swarming insect pests such as the desert locust. We confirmed the prediction of a rapid transition from disordered to ordered movement and identified a critical density for the onset of coordinated marching in locust nymphs. We also demonstrated a dynamic instability in motion at densities typical of locusts in the field, in which groups can switch direction without external perturbation, potentially facilitating the rapid transfer of directional information.

Despite the huge differences in the scales of animal aggregations and the cognitive abilities of group

members, the similarities in the patterns that such groups produce have suggested that general principles may underlie col-

lective motion. One approach has been to model grouping individuals as self-propelled particles (SPPs), with each “particle” adjusting its speed and/or direction in response to near neighbors (1–6). A recent model by Vicsek and collaborators (1) stands out because of its small number of underlying assumptions and the strength of the universal features that it predicts. A central prediction of this model is that as the density of animals in the group increases, a rapid transition occurs from disordered movement of individuals within the group to highly aligned collective motion (Fig. 1). Because SPP models underlie many theoretical predictions about how groups form complex patterns (7–10), avoid predators (11, 12), forage (8, 13), and make decisions (14), confirming the existence of such a transition in real animals has fundamental implications for understanding all aspects of collective motion.

The desert locust, *Schistocerca gregaria*, has a devastating social and economic impact on humans. Before taking flight as adults, wingless juveniles (also called nymphs or hoppers) form coordinated “marching bands” that can extend over many kilometers (15). The key to effective management of locust outbreaks is

early control and detection of bands, because the control of flying adult swarms is costly and ineffective (16). The first stage in band formation is a change among resident locusts from the harmless, non-band-forming “solitarious” phase to the actively aggregating, band-forming “gregarious” phase (17–19).

Previous work has investigated which combinations of locust population density, vegetation abundance, and vegetation distribution will trigger such gregarization (20–23). Locust aggregations will build into major outbreaks only if locally gregarized populations remain together and move collectively into neighboring areas of habitat, where they can recruit further locusts to the growing band. Unless such cohesive movement occurs, local aggregations will disband and individuals will return to the solitarious phase. Hence, it is vital to predict the onset of collective motion. Within bands, individuals align their directions of travel with those of near neighbors (15, 24). Although it has been shown in the laboratory that marching begins only at high locust density (25, 26), these experiments did not measure how alignment increases with density. A detailed quantitative understanding of the onset of collective motion is therefore essential if we are to understand how, when, and where coordinated bands will form, resulting in improved control measures (27).

The average density of marching bands in the field is 50 locusts/m², with a typical range of 20 to 120 locusts/m² (28), equivalent to 20 locusts in our experiments. We performed experiments on different numbers of third-instar locusts,

ranging from 5 to 120 insects (densities of 12.3 to 295 locusts/m²), in a ring-shaped arena (29). We recorded the locusts’ motion for 8 hours with a digital camera placed above the setup and connected to a computer that captured five images/s (see movie S1 for an example). Movies were processed with tracking software that computed the position and orientation of each locust. For each locust, we calculated its angular coordinates relative to the center of the arena on two consecutive camera images. The orientation χ of a locust was defined as the smallest angle between one line drawn between the locust’s two consecutive positions and a second line drawn from the center of the arena to the locust’s first position. This relationship can be described as $\chi = \arcsin[\sin(\theta - \alpha)]$, where α is the angle of the direction of movement and θ is the angle with the center of the arena. For each camera image, or time step t , we calculated the instantaneous alignment Φ^t as the average of the orientation for all moving locusts, normalized as follows

$$\Phi^t = \frac{2}{m\pi} \sum_{i=1}^m \chi_i^t$$

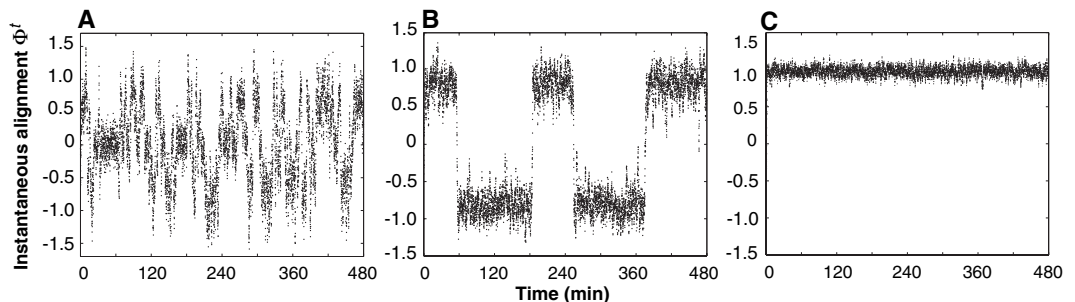
where m is the total number of moving locusts, and i is the i th locust. Thus, values of the alignment close to the extreme values of 1 and -1 indicate the alignment of all locusts in the same direction, whereas values close to zero indicate an absence of any collective alignment. Because locust direction was not influenced by immobile individuals,

¹Department of Zoology, University of Oxford, South Parks Road, Oxford OX1 3PS, UK. ²School of Biological Sciences, Heydon-Laurence Building, A08, University of Sydney, New South Wales 2006, Australia. ³Department of Ecology and Evolutionary Biology, Princeton University, Princeton, NJ 08544–1003, USA.

*To whom correspondence should be addressed. E-mail: jbuhl@usyd.edu.au

†Present address: Biology Department, Concordia University, 7141 Sherbrooke West, Montréal, Québec H4B 1R6, Canada.

Fig. 1. Characteristic output of the model for the dynamics of Φ^t over time and with 3 (A), 11 (B), and 47 (C) individuals. The Vicsek *et al.* SPP model (1) consists of a set of pointwise particles moving synchronously and interacting locally by trying to align with their neighbors (1, 4). We used a variant of the one-dimensional version of their SPP model (30), where N particles move along a line of length L at a discrete time step $\Delta t = 1$. Each particle is characterized by its position x_i and a dimensionless velocity u_i and is updated as follows: $x_i(t + 1) = x_i(t) + v_0 u_i(t)$, $u_i(t + 1) = \alpha u_i(t) + (1 - \alpha)G(\langle u(t) \rangle_i) + \xi_i$, where $\langle u \rangle_i$ denotes the average velocity of all other particles, excluding particle i , within an interaction range $[x_i - \Delta, x_i + \Delta]$. The term α determines the relative weight that the particle assigns to its own velocity and to that of its neighbors in deciding its velocity. For locusts, α corresponds to a directional inertia when walking in the absence of conspecifics. ξ_i is a noise term, randomly chosen with a uniform probability from the interval $[-\eta/2, \eta/2]$. The function G represents the adjustment of a particle velocity to the velocity of its neighbors, implemented as follows



$$G(u) = \begin{cases} (u + 1)/2 & \text{for } u > 0 \\ (u - 1)/2 & \text{for } u < 0 \end{cases}$$

Simulations were run by applying random initial conditions and periodic boundaries. The parameters were set to mimic the walking speed and interaction range of locusts in an arena (see SOM). $T = 8000$ time steps (8 hours), $L = 36$ (251.3 cm), $v_0 = 1$ (1.9 cm/s), $\Delta = 2$ (13.9 cm), $\alpha = 0.66$. The noise term $\eta = 0.8$ was set by trial and error. We used the average velocity $\Phi^t = \langle u(t) \rangle$ as the measure of the order in the system to compare the simulations to the alignment measured experimentally.

and changes of direction occurred mainly as a response to moving neighbors [see the supporting online material (SOM) for details], we considered only the number of moving locusts when calculating densities.

Coordinated marching behavior depended strongly on locust density (Fig. 2). At low densities (2 to 7 moving locusts on average, equating to 5.3 to 17.2 locusts/m²), there was a low incidence of alignment among individuals; in trials where alignment did occur, it did so only sporadically and after long initial periods of disordered motion. Intermediate densities (10 to 25 moving locusts; 24.6 to 61.5 locusts/m²) were characterized by long periods of collective rotational motion with rapid spontaneous changes in direction. At densities above 73.8 locusts/m² (30 or more moving locusts), spontaneous changes in direction did not occur within the time scale of the observations, and the locusts quickly adopted a common and persistent rotational direction (movie S1).

The dynamics of our experiment (Fig. 2, A to C) and that of the SPP model (Fig. 1, A to C) were very similar. To test whether the transition from disordered to ordered marching observed in our experiments was consistent with the predictions of the SPP model, we compared, for different densities, the average Φ^f over the entire experiment with that predicted by an SPP model with parameter values consistent with the behavior of locust

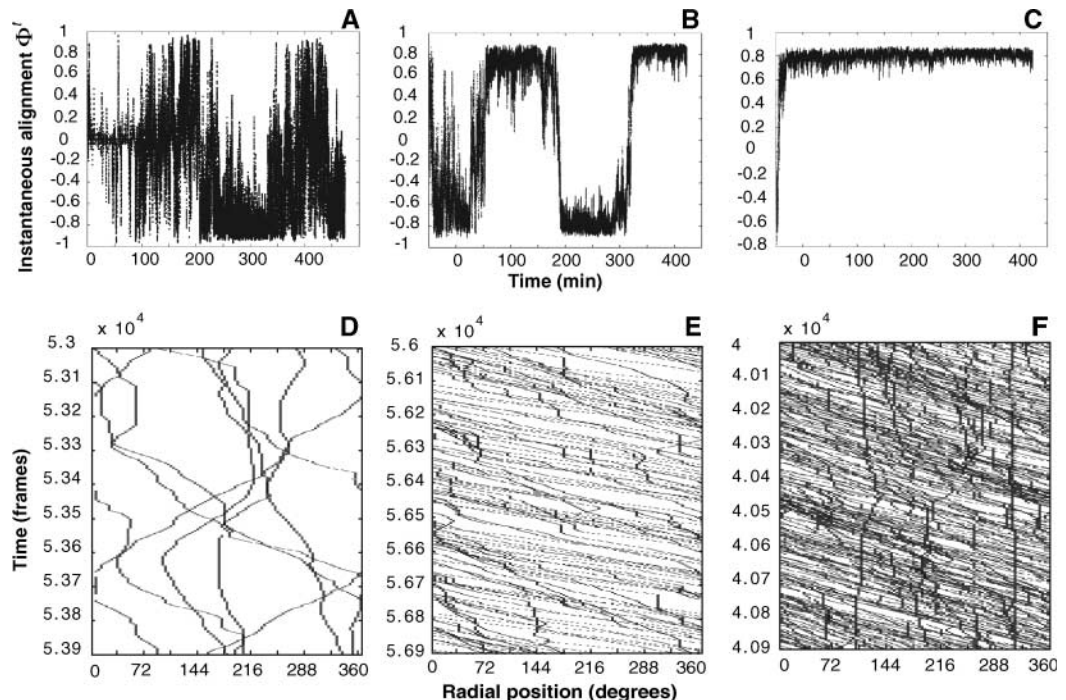
nymphs (Fig. 3, A and D). The mean alignments were very consistent with the distribution of alignment predicted by the model. As density increased, the spread of the alignment changed from a flat distribution to having two well-defined peaks. Rather than being limited to our particular parameterization, such a transition is characteristic of the output of SPP models over a wide range of parameter values (1, 4, 30).

As density increased, the dynamical behavior of the group also exhibited marked changes. The time during which the locusts were aligned increased with increasing density (Spearman's $\rho = 0.782$, $n = 51$, $P < 0.001$) and rapidly saturated at a value corresponding to the total time of the experiment (Fig. 3, B and E). The frequency with which the locusts collectively changed direction decreased with increasing density (Spearman's $\rho = -0.722$, $n = 51$, $P < 0.001$) until it reached a value of zero (Fig. 3, C and F). These two quantities did not saturate at the same densities. Although 10 or more moving locusts (24.6 locusts/m²) were in the ordered phase almost all of the time, it was not until there were at least 30 moving locusts (73.8 locusts/m²) that directional changes dropped to nearly zero. Between these densities, the group was almost always aligned while several directional changes still occurred, indicating that these shifts happened rapidly and without loss in group cohesion. This intermittency in align-

ment is also characteristic of the output of SPP models (31).

At a global level, the behavior of locust groups was fully consistent with the predictions of the SPP model, but did we get the same outcome for different reasons? Detailed observations of the behavior of individual locusts indicate that the mechanisms operating at the level of individual insects are consistent with the core assumptions of the model. The central assumptions of the SPP model are that (i) insects adjust their direction to align with neighbors within an interaction range and (ii) individual behavior does not change with changes in group density. Regarding (i), we observed clear evidence of alignment and chose the interaction range on the basis of detailed analyses of the behavior of locusts in the arena (see SOM). Concerning (ii), we found that the interaction distance did not change with density; the interaction range was 7.58 ± 4.22 SD for the low-density (5 locusts) and 6.24 ± 2.9 SD for the intermediate-density (20 locusts) experiments (two-sample Kolmogorov-Smirnov test: $D^* = 0.09$, $n_1 = 118$, $n_2 = 108$, $P = 0.38$) (see SOM). Similarly, the proportion of active insects, although varying slightly between experimental trials for similar densities, was not related to density (Spearman's $\rho = 0.025$, $n = 51$, $P = 0.862$). As previously reported (25), any given locust spent about half of its time in an active state; the mean proportion of active insects across the group was 0.51 ± 0.11 SD.

Fig. 2. Change in Φ^f over time for three different densities: (A) 7 (or 3.47 moving on average), (B) 20 (or 12.05 moving on average), and (C) 60 (or 47.35 moving on average) locusts. (D to F) Corresponding samples of time-space plots (3 min), where the x axis represents the individuals' angular coordinates relative to the center of the arena, and the y axis represents time.



Inactive insects did not affect the behavior of moving locusts (see SOM). Although there was a significant positive correlation between the mean walking speed of locusts and the number of locusts in the arena (Spearman's $\rho = 0.430$, $n = 51$, $P = 0.002$), it represented only a slight increase (5 locusts, 3.11 ± 0.1 cm/s; 30 locusts, 3.46 ± 0.06 cm/s; 60 to 120 locusts, 3.8 ± 0.08 cm/s). It is known that solitary locusts (those

reared in isolation) increase their activity levels when first exposed to crowding (22). This response is part of the process of behavioral gregarization, which is completed in individuals within a few hours of experiencing crowded conditions (18, 19). Our experiments showed that, within a wide range of densities, once a locust is gregarious there are no further marked changes in its activity.

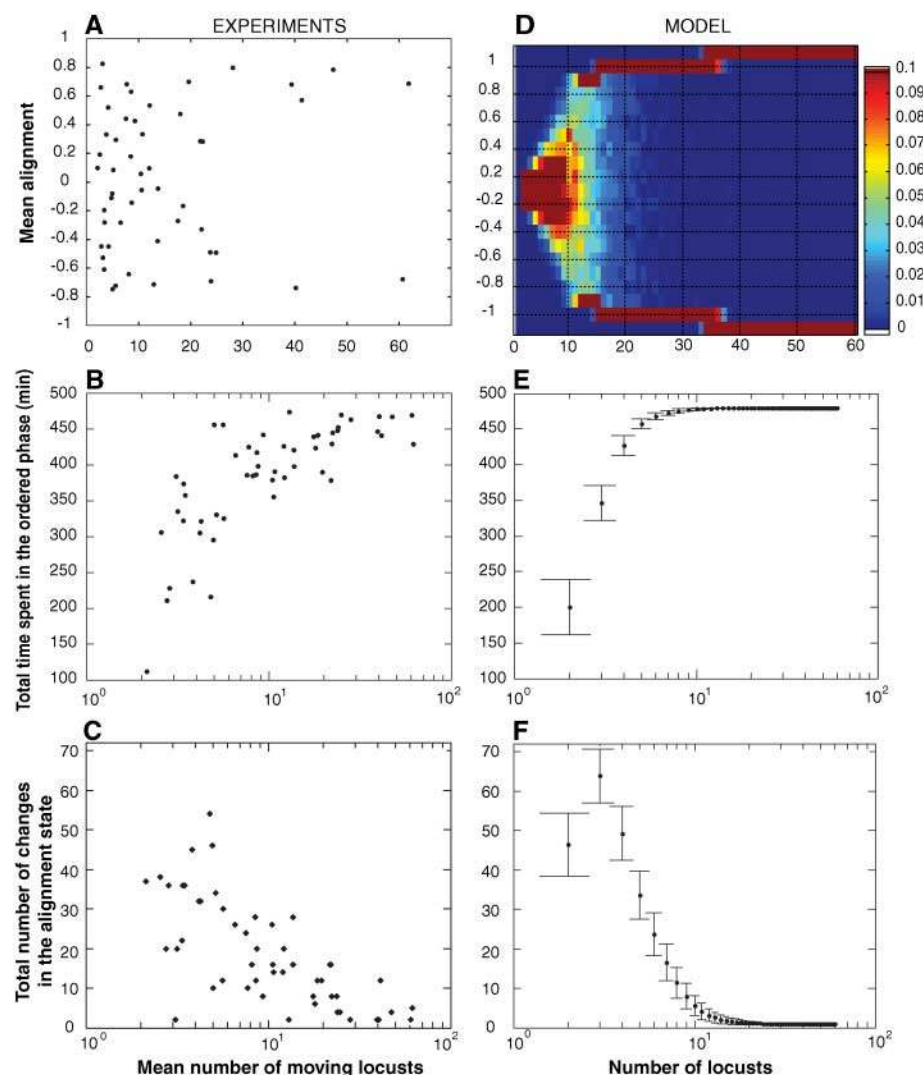


Fig. 3. Changes in alignment with density in experiments (A to C) and the model (D to F). The relation between the number of moving locusts and the mean alignment is shown for the experiments (A) and for simulations (D). Each point in (A) represents one experimental trial, whereas each colored column in (D) shows the distribution of the results obtained for 1000 simulations. To analyze the changes between aligned/unaligned states over time, we considered that locusts belonged to one of three categories: unaligned (alignment value between -0.3 and 0.3), aligned in the counterclockwise direction (alignment value >0.3), or aligned in the clockwise direction (alignment value <-0.3). To remove stochastic noise, the alignment state was only considered to have changed if it persisted for 1 min (16 time steps in the simulation) or more. The relation between the average number of moving locusts and the mean total time spent in the aligned state [(B) and (E)] and the mean number of changes in the alignment state [(C) and (F)] are displayed on a semi-log scale. Error bars, standard deviation.

Both the SPP model and our experiments exhibited dynamic instability, in which changes in direction are sudden and spontaneous, rapidly spreading through the entire group. Such sudden directional changes of locust hoppers and other similar insects such as the Mormon cricket occur in the field (32). Our experiments show that these changes can be independent of external conditions and are likely to be an inherent property of moving groups. These instabilities may have important implications for how directional information is transferred within these groups. For example, if only a subset of a swarm becomes aware of the direction toward a resource, this may facilitate the change in direction over a much greater length scale (14), allowing collective motion along weak environmental gradients that do not elicit responses in individuals alone (13). We predict that at densities of 25 to 60 locusts/m², locust bands are maximally sensitive to such changes in direction. It is unclear, however, whether individual locusts regulate their local density to this level, thereby optimizing their collective access to information about the environment.

We have revealed a critical density at which marching locusts will spontaneously and suddenly adopt directed collective motion. The lower size range of a marching band as defined by the Food and Agriculture Organization of the United Nations (FAO), at 20 locusts/m² (28), corresponds to 8 locusts in our experiments. Because alignment rapidly increases with density around this level, the FAO's definition corresponds to a threshold density for cohesive marching. In our experiments, groups of two to seven moving locusts were only weakly aligned, whereas slightly larger groups changed direction rapidly and in unison. In the field, small increases in density beyond this threshold will cause a sudden transition to a highly unpredictable collective motion, making control measures difficult to implement. Our data and model also suggest that predicting the motion of very high densities of locusts is easier than predicting that of intermediate densities. The small number of directional changes at high densities, observed during the 8 hours of our experiments, was similar to the field observation of "gregarious inertia" that lasts for days (24).

We cannot assume that all of the collective behavior seen in our laboratory experiments translates directly to that observed in the field. However, the wealth of mathematical and simulation-

based understanding of SPP models provides us with tools for performing such scaling. For example, additional rules such as attraction (33) explain how a moving group maintains cohesion in a nonbounded space. In combination with our understanding of the role of the environment in behavioral phase change (20), SPP models could now form the basis of prediction to improve control of locust outbreaks.

References and Notes

1. T. Vicsek, A. Czirók, E. Ben-Jacob, I. Cohen, O. Shochet, *Phys. Rev. Lett.* **75**, 1226 (1995).
2. A. Okubo, *Adv. Biophys.* **22**, 1 (1986).
3. C. W. Reynolds, *Comput. Graphics* **21**, 25 (1987).
4. A. Czirók, H. Stanley, T. Vicsek, *J. Phys. A* **30**, 1375 (1997).
5. J. Toner, Y. Tu, *Phys. Rev. E* **58**, 4828 (1998).
6. G. Grégoire, H. Chaté, *Phys. Rev. Lett.* **92**, 025702 (2004).
7. I. D. Couzin, J. Krause, R. James, G. D. Ruxton, N. R. Franks, *J. Theor. Biol.* **218**, 1 (2002).
8. J. L. Deneubourg, S. Goss, *Ethol. Ecol. Evol.* **1**, 295 (1989).
9. S. Gueron, S. A. Levin, D. I. Rubenstein, *J. Theor. Biol.* **182**, 85 (1996).
10. I. D. Couzin, J. Krause, *Adv. Stud. Behav.* **32**, 1 (2003).
11. W. D. Hamilton, *J. Theor. Biol.* **31**, 295 (1971).
12. J. Parrish, L. Edelstein-Keshet, *Science* **284**, 99 (1999).
13. D. Grunbaum, *Evol. Ecol.* **12**, 503 (1998).
14. I. D. Couzin, J. Krause, N. R. Franks, S. A. Levin, *Nature* **433**, 513 (2005).
15. B. P. Uvarov, *Grasshopper and Locust: a Handbook of General Acridology. Vol. II: Behaviour, Ecology, Biogeography, Population Dynamics* (Cambridge Univ. Press, Cambridge, 1977).
16. M. Enserink, *Science* **306**, 1880 (2004).
17. S. J. Simpson, E. Despland, B. F. Hägele, T. Dodgson, *Proc. Natl. Acad. Sci. U.S.A.* **98**, 3895 (2001).
18. S. J. Simpson, A. R. McCaffery, B. F. Hägele, *Biol. Rev.* **74**, 461 (1999).
19. S. M. Rogers *et al.*, *J. Exp. Biol.* **206**, 3991 (2003).
20. M. Collett, E. Despland, S. J. Simpson, D. C. Krakauer, *Proc. Natl. Acad. Sci. U.S.A.* **95**, 13052 (1998).
21. E. Despland, S. J. Simpson, *Physiol. Entomol.* **25**, 74 (2000).
22. E. Despland, M. Collett, S. J. Simpson, *Oikos* **88**, 652 (2000).
23. E. Despland, J. Rosenberg, S. J. Simpson, *Ecography* **27**, 381 (2004).
24. J. S. Kennedy, *Trans. R. Entomol. Soc. London* **95**, 247 (1945).
25. P. E. Ellis, *Anti-Locust Bull.* **7**, 1 (1951).
26. P. E. Ellis, *Behaviour* **20**, 282 (1961).
27. S. J. Simpson, G. A. Sword, A. De Loof, *J. Orthoptera Res.*, in press.
28. P. M. Symmons, K. Cressman, *Desert Locust Guidelines* (FAO, Rome, 2001; www.fao.org/ag/locusts/common/ecg/347_en_DLG1e.pdf).
29. Materials and methods are available as supporting material on Science Online.
30. A. Czirók, A. Barabási, T. Vicsek, *Phys. Rev. Lett.* **82**, 209 (1999).
31. C. Huepe, M. Aldana, *Phys. Rev. Lett.* **92**, 168701 (2004).
32. P. Lorch, G. Sword, D. Gwynne, G. Anderson, *Ecol. Entomol.* **30**, 548 (2005).
33. G. Grégoire, H. Chaté, Y. Tu, *Physica D* **181**, 157 (2003).
34. We thank T. Dodgson and M. Klapwijk for rearing the locusts and for their invaluable technical expertise, and two anonymous referees for their helpful comments and suggestions. The authors acknowledge support from the Engineering and Physical Sciences Research Council grant GR/S04765/01 (I.D.C., J.B., D.J.T.S., and S.J.S.), the Royal Society (I.D.C., D.J.T.S., and E.D.), Natural Environment Research Council (J.H.), National Sciences and Engineering Research Council Canada (E.D.), the Australian Research Council Federation Fellowship Scheme (S.J.S.), and the ARC Discovery grant DP0664709 (J.B. and S.J.S.).

Supporting Online Material

www.sciencemag.org/cgi/content/full/312/5778/1402/DC1

Materials and Methods

Fig. S1

Table S1

References

Movie S1

19 January 2006; accepted 19 April 2006

10.1126/science.1125142